



# An investigation on sample size in Leeb hardness test and prediction of some index properties of magmatic rocks

Ismail İnce<sup>1</sup> · Ali Bozdağ<sup>1</sup>

Received: 16 May 2020 / Accepted: 5 January 2021 / Published online: 27 January 2021  
© Saudi Society for Geosciences 2021

## Abstract

The first aim of this study is to determine the effect of the sample size on the Leeb hardness (HL), which is a non-destructive test, in magmatic rocks. For this scope, cubic samples with edge lengths of 3, 4, 5, 6, 7, 8, 9, and 10 cm from 15 different magmatic rocks (igneous, volcanic, and pyroclastic) were prepared, and variations of the HL values were measured. Based on the results, it was determined that as the strength values of magmatic rock samples increase, the effect of sample size on HL value decreases. Additionally, the minimum sample size, at which the HL value did not change, was found to be 7 cm. The second aim of this study is to examine the correlation between the HL values of the rocks' minimum sample size, and the index properties were examined by the simple regression method. For this purpose, 76 various types of magmatic rock samples were tested in the laboratory in order to determine their dry and saturated HL values and index (P-wave velocity, dry density, porosity, and uniaxial compressive strength) values. The relationship between the dry and saturated HL values and the index properties of the samples was examined by simple regression analysis. Based on this analysis, a strong linear relationship was found between the index properties. In addition to this, a strong exponential relationship was determined between the dry and saturated HL and uniaxial compressive strength (UCS) values of these rocks, and the determination coefficients ( $R^2$ ) were found to be 0.85 and 0.86, respectively. The Leeb hardness test can be used as a non-destructive method where a regular-shaped rock sample is difficult to obtain (in rocks and/or historical structures) and to estimate the rock properties practically in the laboratory and field.

**Keywords** Leeb hardness · Sample size · Index properties · Simple regression

## Introduction

The Leeb hardness (HL) test is a non-destructive test (NDT) developed by the Swiss engineer Dietmar Leeb in 1975 to provide a portable hardness test originally for metals and polymers. This test uses energy measurement principles in determining the hardness of material (Leeb 1979). The possibility to select the impact direction of the instrument allows the device to be used in both field and laboratory applications (Hack et al. 1993). The use of this method in different areas such as degradation of building stones used in historical buildings (André et al. 2014; Mol and Gomez-Heras 2018;

Wilhelm et al. 2016; Wang et al. 2020), geomorphology (Feal-Pérez and Blanco-Chao 2013; Mol and Viles 2012; Wakasa et al. 2006), civil engineering (Coombes et al. 2013; Kawanishi et al. 2019; Kovler et al. 2018), and rock mechanics has recently become widespread. In rock mechanics, researchers have primarily investigated the relationships between the HL values and index-mechanical and sample size properties of rocks (Alvarez Grima and Babuška 1999; Aoki and Matsukura 2008; Asiri et al. 2016; Corkum et al. 2018; Çelik and Çobanoğlu 2019; Çelik et al. 2020; Lee et al. 2014; Meulenkamp and Grima 1999; Verwaal and Mulder 1993; Viles et al. 2011; Su and Momayez 2017; Yılmaz Güneş and Goktan 2019; Gomez-Heras et al. 2020; Aldeeky et al. 2020). Verwaal and Mulder (1993) conducted a study on 28 different rock (limestone, dolomite, sandstone, marble, granite) samples to investigate the correlation between UCS and HL values of rock samples and the effect of sample size on HL. They found that only the dolomite sample with high porosity did not fit the general correlation trend among other rock samples. Verwaal and Mulder (1993) examined the effect

---

Responsible Editor: Zeynal Abiddin Erguler

✉ İsmail İnce  
iince@ktun.edu.tr

<sup>1</sup> Department of Geological Engineering, Konya Technical University, 42250 Konya, Turkey

of the sample size on the HL value in core samples with diameters of 30, 40, and 50 mm and stated that the HL value was low in samples with a diameter less than 50 mm. Meulenkamp and Grima (1999) used HL, porosity, density, grain size parameters, and lithology of rocks to estimate the UCS value with the neural network method. Alvarez Grima and Babuška (1999) estimated the UCS value of rocks by using multiple regression analysis and the fuzzy method. Aoki and Matsukura (2008) estimated UCS more meaningfully when HL and porosity values were used together, although there was a good correlation between UCS and HL in rocks such as granite, gabbro, andesite, tuff, sandstone, and limestone. Viles et al. (2011) investigated the rock hardness in relation to rock weathering on deteriorated rocks (sandstone, limestone, basalt, and dolerite) by using HL test (standard type D and Piccolo) and Schmidt Hammer (Classic N type and Silver Schmidt BL type). They showed that using Schmidt Hammer and HL tests together may provide crucial information on the structure of shallow depth regions and the nature of deterioration processes. Lee et al. (2014) presented equations for predicting UCS values from HL values where standard-sized specimen is hard to obtain like shale formations. Asiri et al. (2016) also found a reasonable correlation between the UCS and HL values of sandstones in their study. In a study conducted by Corkum et al. (2018), the researchers estimated the relationship between HL and UCS by using data obtained from previous studies and their own data. In this correlation, the  $R^2$  value was determined to be 0.70 for all rocks. The  $R^2$  values according to rock types were determined to be 0.65, 0.79, and 0.71 for igneous, metamorphic, and sedimentary rocks, respectively. These researchers investigated the change in the HL value in core samples with an NX diameter and different lengths (9, 10, 22, 38, 76, 102, 152, and 190.5 mm) and in cubic sandstone samples with different edge lengths (25, 51, 102, and 203 mm), and, as a result of the tests conducted, they stated that the HL value became stable in samples with a volume larger than  $90 \text{ cm}^3$  (Asiri 2017; Asiri et al. 2016; Corkum et al. 2018). Su and Momayez (2017) investigated the relationship between HL value, mechanical properties, Shore hardness, and drilling rate index of rocks by using simple regression analysis. They also stated that the brittleness property and drilling rate index of rock can be determined by using HL values. Yilmaz Güneş and Goktan (2019) estimated the UCS values by using the Schmidt hammer and Leeb hardness methods separately and together. They stated that the UCS values could be estimated better by using the Schmidt hammer and Leeb hardness methods together. Çelik and Çobanoğlu (2019) reported that the Leeb hardness test is more useful in estimating the physical and mechanical properties of rocks due to its fast, accurate, and safe measurement capacity compared with the Shore and Schmidt hardness tests. Çelik et al. (2020) stated that there is a remarkable exponential relationship between the HL value

and saturated weight per unit of volume, porosity, and UCS values in rock such as ignimbrite, travertine, and syenite. The study investigated the effect of the sample size on the HL value in core samples with an NX diameter (54 mm) and different lengths (25, 50, 75, 100, and 125 mm) and stated that the HL value increased linearly with an increase in the core volume. Aldeeky et al. (2020) investigated the relationships between UCS and Young's modulus of basalt rock using the HL test. They found a strong power correlation ( $R^2 = 0.888$ ) between non-destructive HL value and UCS and a strong linear regression ( $R^2 = 0.792$ ) between Young's modulus and HL. Gomez-Heras et al. (2020) carried out a simple and multiple regression analysis to develop a predictive model of UCS from NDT method (HL and P-wave velocity). Gomez-Heras et al. (2020) showed that integrating HL ( $R^2 = 0.951$ ) with HL and P-wave velocity ( $R^2 = 0.956$ ) did not affect the quality of overall HL values in UCS estimation for a large set of rock samples (including sedimentary, magmatic, and metamorphic). These researchers, on the other hand, showed that in low porosity rocks, the effect in UCS estimation integrating NDT methods gives better results ( $R^2: 0.816$ ,  $R^2: 0.779$ ).

The determination of minimum values by detecting the effect of the sample size on the HL value of rocks is of great importance in terms of ensuring the suitability and usability of the standards to be developed for rocks. In the stage of this study, it was aimed to determine the change in the HL values in cubic samples with an edge length varying between 3 and 10 cm of 15 magmatic rock (igneous, volcanic, and pyroclastic) samples with index and strength values changing in a wide range and to determine the most appropriate sample size. It is essential to understand the relationship between the HL values of rocks in dry and saturated states and their engineering properties. The aim of the second stage of this study is to determine the index values of 76 magmatic rock (plutonic, volcanic, and pyroclastic) samples by using the Leeb hardness test method.

## Material and methods

A total of 15 magmatic rock samples for determination of the effect of the sample size on the HL value and 76 magmatic rock samples for examination of the relationship between the HL values of the rocks' minimum sample size and the index properties were collected from the Anatolia, Turkey. The samples' locations, rock lithologies, petrographic analysis, and mean particle size are shown in Tables 1 and 2.

### Leeb hardness test

Although there is a standard method of the Leeb hardness test for steel products (ASTM A956 2012), there is currently no

**Table 1** The location and type of the rock samples (samples of size effect)

| Sample | Location               | Rock lithologies | Mean particle size |
|--------|------------------------|------------------|--------------------|
| P1     | Kaman/Kırşehir         | Plutonic         | Very coarse        |
| P2     | Unknown-1              | Plutonic         | Medium             |
| P3     | Ispir/Erzurum          | Plutonic         | Medium             |
| P4     | Unknown-2              | Plutonic         | Coarse             |
| P5     | Bergama/İzmir          | Plutonic         | Medium             |
| Py1    | Kayseri-1              | Pyroclastic      | Fine               |
| Py2    | Karayazı-1/Neveşehir   | Pyroclastic      | Very coarse        |
| Py3    | Kayseri-2              | Pyroclastic      | Fine               |
| Py4    | Kayseri-3              | Pyroclastic      | Coarse             |
| Py5    | Karayazı-2/Neveşehir   | Pyroclastic      | Medium             |
| V1     | Erkilet-1/Kayseri      | Volcanic         | Fine               |
| V2     | Kayseri-6              | Volcanic         | Fine               |
| V3     | Sivrihisar-1/Eskişehir | Volcanic         | Medium             |
| V4     | Isparta                | Volcanic         | Coarse             |
| V5     | Sille-1/Konya          | Volcanic         | Coarse             |

Mean particle size: fine (< 1 mm), medium (1–5 mm), coarse (5 mm–3 cm), very coarse (> 3cm)

universally established standard for rock materials. HL value measurements were made using the D-probe of the Insize ISH-PHB test device. Some technical features of the device are as follows: measurement range (0 to 999 HL), impact energy (11 Nmm), and accuracy ( $\pm 6$  HL). Before the HL value was determined, the calibration of the instrument was performed, and 20 different points of impact were selected evenly distributed on a surface of a cubic sample, and the arithmetic mean of these values was determined as the HL value for a sample.

In the first stage of this study, 120 rock samples were prepared from 15 rock specimens consisting of plutonic (P1–P5), pyroclastic (Py1–Py5), and volcanic (V1–V5) rocks with length dimensions of 3, 4, 5, 6, 7, 8, 9, and 10 cm (Fig. 1). The samples were dried in the oven at 100 °C for 24 hours. Then, HL values of the samples were determined.

In the second stage of this study, the HL measurements in of cube samples with an edge length of 7 cm were made. At this stage, 8 plutonic (P6–P13), 25 pyroclastic (Py6–Py30), and 28 volcanic (V6–V33) rock samples were added to the rock samples used in the first stage of the study (Table 2). The HL measurements were made on both dry and saturated samples. The HL values measured after drying the samples in the oven at 100 °C for 24 hours and cooling them at room temperature were defined as the dry Leeb hardness ( $HL_D$ ) value. The values measured after the samples were saturated with distilled water for 48 hours were determined as the saturated Leeb hardness ( $HL_S$ ) value.

## Index properties

Test specimens were prepared in accordance with the pertinent standards and suggested test methods (TS EN-1936 2010; ASTM E494 2010) in order to ascertain their relevant physical properties (dry density, porosity, and P-wave velocity).

## Uniaxial compressive strength tests

The UCS tests were performed on cubic samples with an edge length of 70 mm (TS EN-1926 2007). The loading rate within the limits of  $1.0 \pm 0.5$  MPa/s was applied. The UCS tests were run five times for each rock sample, and the average UCS value of each specimen was determined.

## Evaluations of test results and conclusions

### Evaluations of sample size on HL measurements

The change in the HL values depending on the sample size of the rocks used in this study is shown in Table 3. In plutonic rocks, the HL value was determined to be similar in samples with an edge length of 5–10 cm (Fig. 2a). Furthermore, although the standard deviation values of HL measurements are low across plutonic rocks (samples P2–P5), the standard deviation values of HL measurements are high in sample P1 (Table 3). The strength values are affected depending on the change in the percentage of orthoclase phenocrystson the failure surface of rocks (Fener and Ince 2012). Similarly, high standard deviations in the HL value of this rock can be explained by the change in the percentage of orthoclase phenocrystson (with very coarse of mean particle size), the surface to which the test is applied (Fig. 3a).

HL values were observed to be very close in each sample group with edge lengths between 7 and 10 cm among pyroclastic rock samples (Fig. 2b). However, it was determined that HL values generally decreased significantly as the sizes of samples with an edge length lower than 7 cm decreased. Nevertheless, only in sample Py2, no regular change in the HL value was detected with the size change. The reason for this can be explained by the fact that different particle size rock fragments observed in the composition of sample Py2 affect the HL value of the rock directly (Fig. 3b).

Finally, in volcanic rock samples, it is observed that the HL value is close in samples with an edge length greater than 6 cm (Fig. 2c). The HL value tends to decrease in samples with an edge length less than 6 cm. In such samples, a significant decrease in the HL value was observed in samples with an edge length of 3 cm.

As the strength value of rocks increases, the rate of samples being affected by the sample size decreases. In general, HL

**Table 2** The location and type of the rock samples (all of sample)

| Sample | Location               | Rock lithologies | Mineralogical composition                              | Rock name                        |
|--------|------------------------|------------------|--|----------------------------------|
| P1     | Kaman/Kırşehir         | Plutonic         | O: 33, P: 24, Q: 18, A: 15, B: 5, Om: 2                | Granite <sup>a</sup>             |
| P2     | Unknown-1              | Plutonic         | O: 60, Q: 18, B: 12, P: 10                             | Granite <sup>a</sup>             |
| P3     | Ispir/Erzurum          | Plutonic         | O: 33, P: 32, Q: 20, A: 14, Om: 1                      | Granite <sup>a</sup>             |
| P4     | Unknown-2              | Plutonic         | O: 40, Q: 25, P: 19, B: 5, Prx: 3, A: 2                | Granite <sup>a</sup>             |
| P5     | Bergama/İzmir          | Plutonic         | O: 45, Q: 23, P: 20, B: 10, Om: 2                      | Granite <sup>a</sup>             |
| P6     | Ulaş/Kırıkkale         | Plutonic         | P: 30, A: 26, Q: 24, O: 15, B: 4, Om: 1                | Granite <sup>a</sup>             |
| P7     | Yaylak/Aksaray         | Plutonic         | Q: 31, P: 29, O: 22, B: 14, A: 3, Om: 1                | Granite <sup>a</sup>             |
| P8     | Unknown-3              | Plutonic         | O: 35, A: 25, Q: 21, P: 19                             | Granite <sup>a</sup>             |
| P9     | Unknown-4              | Plutonic         | O: 35, P: 27, Q: 16, A: 12, B: 8, Om: 2                | Granite <sup>a</sup>             |
| P10    | Unknown-5              | Plutonic         | O: 39, Q: 27, P: 23, A: 9, Om: 2                       | Granite <sup>a</sup>             |
| P11    | Aksaray                | Plutonic         | Q: 33, P: 30, O: 25, B: 8, A: 2, Om: 2                 | Granite <sup>a</sup>             |
| P12    | Çanakkale              | Plutonic         | P: 29, Q: 23, O: 20, B: 16, A: 10, Om: 2               | Granite <sup>a</sup>             |
| P13    | Unknown-6              | Plutonic         | P: 48, Ol: 40, Prx: 10, Om: 2                          | Gabro <sup>a</sup>               |
| Py1    | Kayseri-1              | Pyroclastic      | Vg: 70, P: 25, B: 3, Om: 1                             | Vitric tuff <sup>b</sup>         |
| Py2    | Karayazı-1/Nevşehir    | Pyroclastic      | Rf: 46, Vg: 37, P: 14, A: 2, Om: 1                     | Lithic tuff <sup>b</sup>         |
| Py3    | Kayseri-2              | Pyroclastic      | Vg: 80, P: 15, Prx: 2, Om: 1                           | Vitric tuff <sup>b</sup>         |
| Py4    | Kayseri-3              | Pyroclastic      | Vg: 60, P: 20, Rf: 14, Q: 2, Prx: 2, Om: 2             | Vitric tuff <sup>b</sup>         |
| Py5    | Karayazı-2/Nevşehir    | Pyroclastic      | Vg: 76, P: 7, A: 3, Q: 2, Om: 1                        | Vitric tuff <sup>b</sup>         |
| Py6    | Demirciler/Aksaray     | Pyroclastic      | Vg: 46, P: 25, B: 10, Rf: 9, Q: 9, Om: 1               | Vitric tuff <sup>b</sup>         |
| Py7    | Selime/Aksaray         | Pyroclastic      | Vg: 53, P: 23, Rf: 9, Q: 9, B: 5, Om: 1                | Vitric tuff <sup>b</sup>         |
| Py8    | Gümüşler/Niğde         | Pyroclastic      | Vg: 68, P: 13, Rf: 7, Q: 6, B: 5, Om: 1                | Vitric tuff <sup>b</sup>         |
| Py9    | Koçcağız/Kayseri       | Pyroclastic      | Vg: 79, P: 9, Rf: 5, Q: 5, B: 1, Om: 1                 | Vitric tuff <sup>b</sup>         |
| Py10   | Kuruköprü/Kayseri      | Pyroclastic      | Vg: 60, P: 11, S: 8, Q: 8, Rf: 4, B: 3, Om: 1          | Vitric tuff <sup>b</sup>         |
| Py11   | Emmiler/Kayseri        | Pyroclastic      | Vg: 51, P: 19, Rf: 11, Prx: 6, S: 5, Q: 4, B: 3, Om: 1 | Vitric tuff <sup>b</sup>         |
| Py12   | Tomarza/Kayseri        | Pyroclastic      | Vg: 63, Rf: 23, P: 14                                  | Vitric tuff <sup>b</sup>         |
| Py13   | Karayazı-3/Nevşehir    | Pyroclastic      | Vg: 65, P: 14, Q: 12, Rf: 8, Om: 1                     | Vitric tuff <sup>b</sup>         |
| Py14   | Ahlat/Bitlis           | Pyroclastic      | Vg: 60, P: 23, Rf: 10, Prx: 4, Q: 2, Om: 1             | Vitric tuff <sup>b</sup>         |
| Py15   | Karayazı-4/Nevşehir    | Pyroclastic      | Vg: 78, P: 10, Q: 6, Rf: 4, Om: 2                      | Vitric tuff <sup>b</sup>         |
| Py16   | Karayazı-5/Nevşehir    | Pyroclastic      | Vg: 60, P: 25, Rf: 8, B: 3, Q: 3, Om: 1                | Vitric tuff <sup>b</sup>         |
| Py17   | Kayseri-4              | Pyroclastic      | Vg: 53, P: 18, Rf: 5, Prx: 7, A: 8, B: 8, Om: 1        | Vitric tuff <sup>b</sup>         |
| Py18   | Mimarsinan/Kayseri     | Pyroclastic      | Vg: 50, P: 28, Rf: 9, Prx: 7, A: 5, Om: 1              | Vitric tuff <sup>b</sup>         |
| Py19   | Turanlar/Kayseri       | Pyroclastic      | Vg: 56, P: 25, Prx: 13, Rf: 3, A: 2, Om: 1             | Vitric tuff <sup>b</sup>         |
| Py20   | Gökyurt/Konya          | Pyroclastic      | Vg: 38, P: 29, A: 13, Rf: 12, B: 7, Om: 1              | Crystal tuff <sup>b</sup>        |
| Py21   | Kayseri-5              | Pyroclastic      | Vg: 50, P: 34, A: 7, B: 5, Rf: 3 Om: 1                 | Vitric tuff <sup>b</sup>         |
| Py22   | Aksaray                | Pyroclastic      | Vg: 70, P: 18, A: 6, Rf: 3, B: 2, Om: 1                | Vitric tuff <sup>b</sup>         |
| Py23   | Kızılören/Konya        | Pyroclastic      | Vg: 75, Rf: 17, P: 8                                   | Vitric tuff <sup>b</sup>         |
| Py24   | Ardıçlı-1/Konya        | Pyroclastic      | P: 25, Rf: 18, Q: 13, A: 8, B: 5, Om: 1, SC: 30        | Crystal tuff <sup>b</sup>        |
| Py25   | Ayazini/Afyonkarahisar | Pyroclastic      | Vg: 68, Q: 20, P: 10, B: 2                             | Vitric tuff <sup>b</sup>         |
| Py26   | Konya                  | Pyroclastic      | Vg: 50, P: 24, A: 12, Rf: 7, B: 5, Om: 1               | Vitric tuff <sup>b</sup>         |
| Py27   | Ardıçlı-2/Konya        | Pyroclastic      | P: 25, Rf: 15, Q: 9, A: 5, B: 5, Om: 1, SC: 40         | Crystal tuff <sup>b</sup>        |
| Py28   | Küçükmuhsine/Konya     | Pyroclastic      | Vg: 57, Rf: 31, P: 9, Q: 3                             | Vitric tuff <sup>b</sup>         |
| Py29   | Gülşehir/Aksaray       | Pyroclastic      | Vg: 66, P: 23, B: 10, Om: 1                            | Vitric tuff <sup>b</sup>         |
| Py30   | Nevşehir               | Pyroclastic      | Vg: 56, P: 20, Rf: 18, Prx: 5, Om: 1                   | Vitric tuff <sup>b</sup>         |
| V1     | Erkilet-1/Kayseri      | Volcanic         | Pm: 55, Prx: 24, Ol: 13, P: 8, Om: 1                   | Basalt <sup>a</sup>              |
| V2     | Kayseri-6              | Volcanic         | Pm: 48, Prx: 34, P: 17, Om: 1                          | Andesite <sup>a</sup>            |
| V3     | Sivrihisar-1/Eskişehir | Volcanic         | Pm: 45, P: 23, Vg: 15, A: 10, Prx: 5, Om: 2            | Andesite <sup>a</sup>            |
| V4     | Isparta                | Volcanic         | Pm: 50, P: 15, Prx: 10, B: 10, N: 10, S: 5,            | Phonolitic-basanite <sup>a</sup> |
| V5     | Sille-1/Konya          | Volcanic         | Vg: 33, P: 22, Pm: 20, Q: 13, B: 10, Om: 2             | Dacite <sup>a</sup>              |
| V6     | Adakale-1/Konya        | Volcanic         | Vg: 52, P: 22, A: 20, Q: 4, B: 1, Om: 1                | Quartz andesite <sup>a</sup>     |

**Table 2** (continued)

| Sample | Location                 | Rock lithologies | Mineralogical composition                          | Rock name                    |
|--------|--------------------------|------------------|--|------------------------------|
| V7     | Adakale-2/Konya          | Volcanic         | Vg: 39, A: 30, P: 20, Pm: 10, Om: 1                | Andesite <sup>a</sup>        |
| V8     | Madenşehir-1/Karaman     | Volcanic         | Vg: 20, Pm: 28, P: 18, Prx: 15, A: 15, B: 3, Om: 1 | Andesite <sup>a</sup>        |
| V9     | Madenşehir-2/Karaman     | Volcanic         | Vg: 32, Pm: 21, P: 18, A: 18, Prx: 9, B: 1         | Andesite <sup>a</sup>        |
| V10    | Niğde                    | Volcanic         | Vg: 23, Pm: 23, P: 20, A: 15, B: 13, Q: 5, Om: 1   | Andesite <sup>a</sup>        |
| V11    | Karaali/Konya            | Volcanic         | Vg: 30, Pm: 20, P: 20, Q: 19, Om: 1                | Quartz andesite <sup>a</sup> |
| V12    | Fasıllar/Konya           | Volcanic         | Pm: 30, V: 27, P: 18, A: 15, B: 6, Q: 3, Om: 1     | Andesite <sup>a</sup>        |
| V13    | Orta/Çankırı             | Volcanic         | Pm: 39, P: 28, A: 22, B: 10, Om: 1                 | Andesite <sup>a</sup>        |
| V14    | Sille-2/Konya            | Volcanic         | P: 26, Vg: 23, B: 17, Pm: 18, Q: 15, Om: 1         | Quartz andesite <sup>a</sup> |
| V15    | Eskişehir                | Volcanic         | Pm: 54, A: 20, Prx: 12, P: 10, C: 3, Om: 1         | Andesite <sup>a</sup>        |
| V16    | Kulu/Konya               | Volcanic         | P: 24, Prx: 23, Vg: 20, Pm: 18, A: 15, Om: 1       | Andesite <sup>a</sup>        |
| V17    | Gölbaşı-1/Ankara         | Volcanic         | Pm: 41, P: 25, A: 20, Prx: 13, Om: 1               | Andesite <sup>a</sup>        |
| V18    | Gölbaşı-2/Ankara         | Volcanic         | P: 25, Vg: 24, Pm: 20, Prx: 18, A: 12, Om: 1       | Andesite <sup>a</sup>        |
| V19    | Kayseri-7                | Volcanic         | P: 28, Vg: 25, Pm: 23, A: 23, Om: 1                | Andesite <sup>a</sup>        |
| V20    | İscehisar/Afyonkarahisar | Volcanic         | Pm: 54, Prx: 32, B: 10, P: 2, Om: 2                | Andesite <sup>a</sup>        |
| V21    | Sincan/Ankara            | Volcanic         | Vg: 30, P: 25, Pm: 20, A: 17, B: 6, Om: 2          | Andesite <sup>a</sup>        |
| V22    | Sivrihisar-2/Eskişehir   | Volcanic         | Pm: 59, Prx: 20, P: 15, A: 5, Om: 1                | Andesite <sup>a</sup>        |
| V23    | Sivrihisar-3/Eskişehir   | Volcanic         | Pm: 54, A: 18, P: 15, Prx: 12, Om: 1               | Andesite <sup>a</sup>        |
| V24    | Hisar, Kulu-1/Konya      | Volcanic         | P: 25, A: 25, Pm: 24, Vg: 20, Prx: 5, Om: 1        | Andesite <sup>a</sup>        |
| V25    | Hisar, Kulu-2/Konya      | Volcanic         | Pm: 30, Vg: 24, A: 20, Prx: 5, Om: 1               | Andesite <sup>a</sup>        |
| V26    | YunusEmre/Manisa         | Volcanic         | P: 30, Vg: 23, A: 22, Prx: 5, B: 3, Om: 2, SQ: 15  | Andesite <sup>a</sup>        |
| V27    | Çayırılı/Ankara          | Volcanic         | Pm: 64, A: 20, P: 15, Om: 1                        | Andesite <sup>a</sup>        |
| V28    | Yunt/Manisa              | Volcanic         | Vg: 39, P: 25, A: 20, Prx: 10, Pm: 5, Om: 1        | Andesite <sup>a</sup>        |
| V29    | İnsuyu/Kayseri           | Volcanic         | Pm: 54, Prx: 30, P: 15, Om: 1                      | Andesite <sup>a</sup>        |
| V30    | Seydişehir/Konya         | Volcanic         | Vg: 28, P: 27, Pm: 20, A: 18, B: 5, Om: 2          | Andesite <sup>a</sup>        |
| V31    | Erzurum                  | Volcanic         | P: 35, Vg: 33, Pm: 20, A: 10, Om: 2                | Andesite <sup>a</sup>        |
| V32    | Gölbaşı-3-Ankara         | Volcanic         | P: 30, Vg30, Prx: 17, Pm: 15, A: 7, Om: 1          | Andesite <sup>a</sup>        |
| V33    | Erkilet-2/Kayseri        | Volcanic         | Pm: 60, Prx: 23, Ol: 12, P: 5, Om: 1               | Basalt <sup>a</sup>          |

A amphibole, B biotite, C calcite, N nepheline, O orthoclase, Ol olivine, Om opaque mineral, P plagioclase, Pm plagioclase microlite, Prx pyroxene, Rf rock fragment, Q quartz, SC secondary calcite, SQ secondary quartz, Vg volcanic glass

<sup>a</sup> Rock names given according to Streickeisen (1979)

<sup>b</sup> Rock names given according to Schmid (1981)

values increase with the increasing size of rocks subjected to the experiment (with an increase in the edge length) and reach a constant Leeb hardness value at the minimum sample size depending on the type of the rock used in the experiment. In

this study, the minimum edge length was determined as 7 cm for magmatic rocks. The amplitude of fluctuations in HL value increases as the grain size of the rocks increases. Figure 4 was prepared to control the reliability of the minimum edge

**Fig. 1** Cubic samples with different edge lengths (between 3 and 10 cm) prepared for determining the sample size



**Table 3** Leeb hardness values depending on the sample size (mean value)

| Sample no. | Specimen edge length (cm) |                |                |                |                |                |               |               |
|------------|---------------------------|----------------|----------------|----------------|----------------|----------------|---------------|---------------|
|            | 3                         | 4              | 5              | 6              | 7              | 8              | 9             | 10            |
| P1         | 669.87 ± 51.4             | 746.53 ± 57.3  | 777.07 ± 83.2  | 781.13 ± 88.7  | 802.27 ± 72.9  | 787.47 ± 71.6  | 810.60 ± 74.3 | 828.53 ± 63.5 |
| P2         | 754.53 ± 28.7             | 810.27 ± 57.9  | 852.20 ± 20.3  | 888.93 ± 20.3  | 872.27 ± 22.0  | 884.27 ± 21.6  | 866.47 ± 35.2 | 892.80 ± 24.7 |
| P3         | 757.40 ± 39.6             | 841.47 ± 19.4  | 866.40 ± 25.6  | 878.67 ± 20.7  | 889.40 ± 27.6  | 890.71 ± 19.6  | 892.00 ± 13.9 | 902.40 ± 17.4 |
| P4         | 746.47 ± 48.6             | 819.60 ± 30.3  | 827.93 ± 38.4  | 871.67 ± 17.2  | 881.47 ± 20.1  | 873.00 ± 13.5  | 874.07 ± 32.0 | 881.33 ± 27.0 |
| P5         | 680.13 ± 43.6             | 748.07 ± 52.2  | 796.67 ± 31.8  | 793.60 ± 32.4  | 825.13 ± 27.8  | 821.93 ± 35.3  | 817.13 ± 28.9 | 816.87 ± 34.1 |
| Py1        | 264.53 ± 61.2             | 379.20 ± 16.4  | 400.07 ± 41.7  | 419.53 ± 19.6  | 451.93 ± 28.4  | 451.47 ± 27.1  | 451.00 ± 26.9 | 446.60 ± 26.9 |
| Py2        | 310.33 ± 87.9             | 511.80 ± 131.4 | 565.13 ± 185.4 | 465.33 ± 122.2 | 501.27 ± 104.1 | 507.20 ± 122.7 | 518.07 ± 72.2 | 522.53 ± 92.4 |
| Py3        | 463.00 ± 80.2             | 545.60 ± 78.4  | 565.33 ± 47.2  | 561.80 ± 47.2  | 610.33 ± 43.4  | 609.53 ± 37.9  | 622.07 ± 40.6 | 611.40 ± 31.5 |
| Py4        | 215.07 ± 36.3             | 230.27 ± 52.3  | 276.13 ± 29.1  | 330.87 ± 57.1  | 383.53 ± 22.3  | 373.60 ± 25.3  | 385.60 ± 28.4 | 382.80 ± 27.3 |
| Py5        | 180.40 ± 24.4             | 234.80 ± 22.7  | 262.93 ± 31.8  | 281.00 ± 29.2  | 300.33 ± 41.6  | 303.40 ± 20.0  | 308.13 ± 25.1 | 317.73 ± 22.9 |
| V1         | 544.13 ± 67.9             | 677.67 ± 72.4  | 664.00 ± 84.9  | 726.20 ± 46.9  | 781.53 ± 30.0  | 772.53 ± 25.9  | 789.67 ± 21.2 | 783.87 ± 30.7 |
| V2         | 616.60 ± 61.8             | 732.80 ± 66.9  | 744.40 ± 54.1  | 748.80 ± 37.9  | 800.93 ± 24.2  | 802.53 ± 34.8  | 799.73 ± 21.8 | 801.20 ± 17.7 |
| V3         | 575.80 ± 55.7             | 657.87 ± 65.6  | 636.87 ± 83.7  | 686.73 ± 73.8  | 713.93 ± 28.2  | 716.87 ± 34.1  | 712.60 ± 31.9 | 711.93 ± 35.7 |
| V4         | 599.93 ± 66.8             | 707.33 ± 52.3  | 739.20 ± 53.1  | 768.93 ± 45.6  | 809.00 ± 59.6  | 802.13 ± 31.8  | 801.53 ± 49.8 | 806.67 ± 45.6 |
| V5         | 461.13 ± 129.4            | 543.07 ± 69.8  | 551.87 ± 83.9  | 614.47 ± 70.6  | 651.67 ± 35.6  | 651.20 ± 27.7  | 650.67 ± 34.6 | 650.73 ± 28.0 |

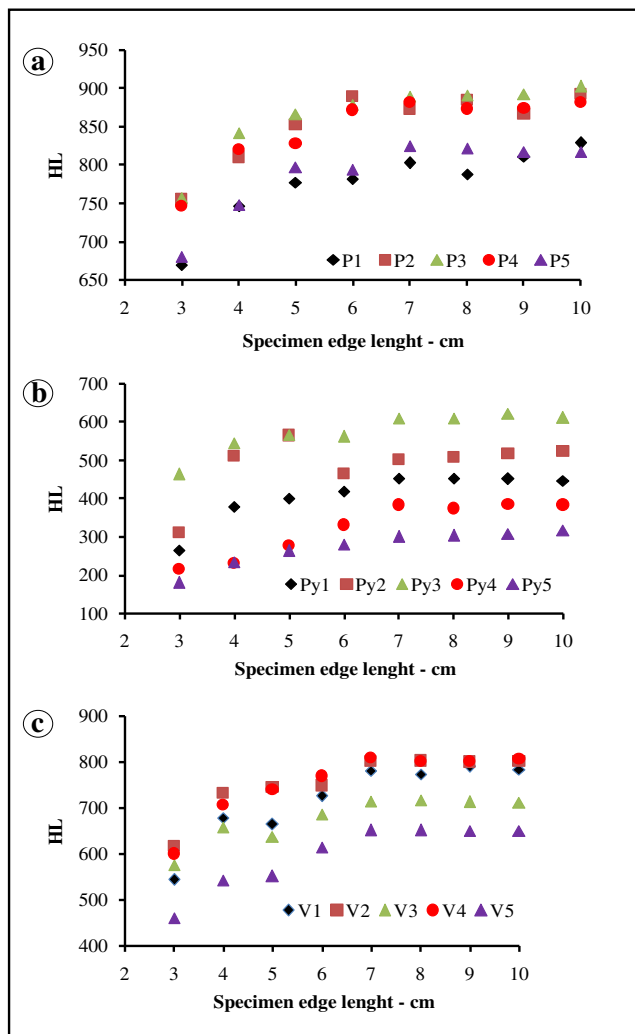


**Fig. 2** Changes in HL values according to the sample size: **a** plutonic rocks, **b** pyroclastic rocks, and **c** volcanic rocks

length value determined for magmatic rocks. Upon examining Fig. 4, it was determined that the HL value was not affected by the sample size above the minimum edge length.

**Correlations of HL and index properties of samples**

The index properties (dry density, porosity, P-wave velocity, and uniaxial compressive strength) and HL values of the magmatic rocks used in this study are presented in Table 4. The results of statistical analysis obtained from the above mentioned data are given in Table 5.

The dry densities of the magmatic rocks tested in this study vary between 1.23 and 2.85 g/cm<sup>3</sup>, while porosity values range between 0.85 and 37.36%. According to dry density classification of NBG (1985), these rock samples are in the very low to high rock classes. On the other hand, the magmatic rock samples are in the range of low to very high classes based on NBG (1985) porosity classification.

The highest P-wave velocity was measured to be 5.43 km/s in the granitoid sample of no P5, and the lowest P-wave velocity was measured to be 1.56 km/s on the pyroclastic sample Py24. The magmatic rock samples with strength values varying in a wide range were examined. The UCS values of the rock samples varied between 7.57 and 194.60 MPa. While the UCS values of the volcanic and plutonic rocks were classified as the moderate to high rock classes, the pyroclastic rocks varied between the low and high classes based on the Bieniawski (1989) classification. While the HL<sub>D</sub> values of the samples used in this study ranged between 220.00 and 895.40, the HL<sub>S</sub> values ranged between 179.40 and 868.00. While the lowest HL<sub>D</sub> and HL<sub>S</sub> values were determined in pyroclastic rocks, the highest HL<sub>D</sub> and HL<sub>S</sub> values were established in plutonic rocks. The HL values determined in

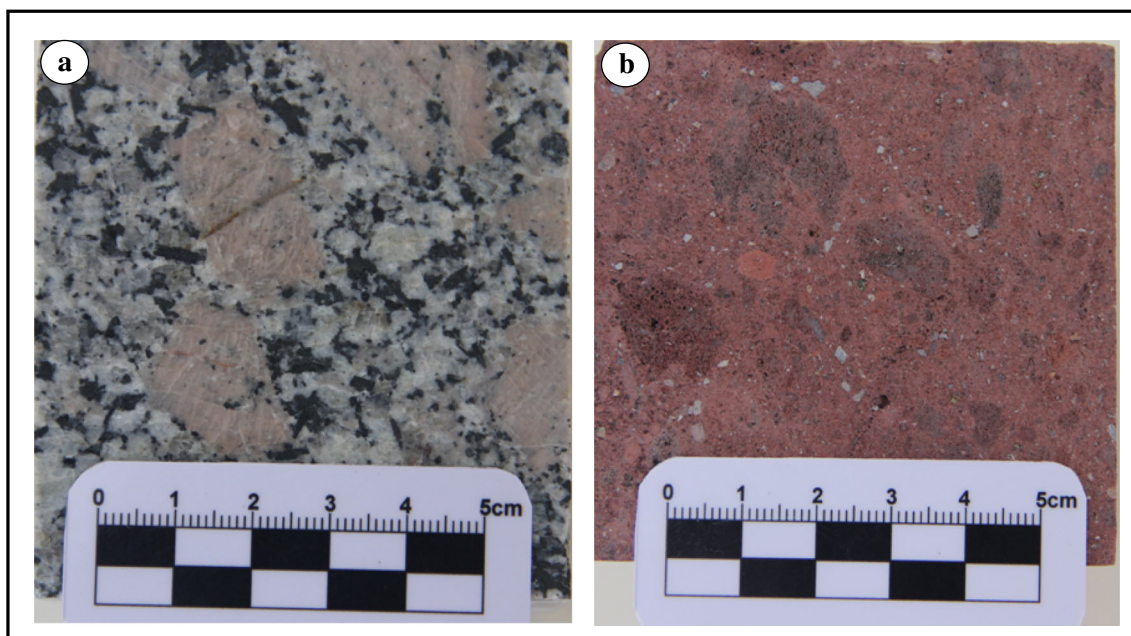


Fig. 3 Factors affecting the HL value: a orthoclase phenocrysts and b volcanic rock fragments

dry samples were higher than the HL values determined in saturated samples (Fig. 5). Figure 5 indicates that the smallest difference between  $HL_D$  and  $HL_S$  values was observed in granitoids, while the biggest difference was observed in pyroclastic rocks. This can be explained by the water absorption capacity of rocks.

The relationships between the index (dry density, porosity, P-wave velocity, and UCS) values of magmatic rocks and their HL values were examined by simple regression analysis (linear, power, exponential, logarithmic, and quadratic). The validity of the derived equations was checked by the  $t$ - and  $F$ -tests. If the computed  $t$ - and  $F$ -values are higher than those tabulated, the null hypothesis is not rejected. This result shows that the  $R^2$  value is significant. If the computed  $t$ - and  $F$ -values

are lower than those of the tabulated values, the null hypothesis is rejected. The computed values are higher than the tabulated  $t$ - and  $F$ -values, showing that the models in the study are valid. For the reliability of the developed equations for a 5% significance level ( $\alpha = 0.05$ ), the  $p$ -value is required to be less than 0.05. In determining the best equation among those that fulfil this condition, the equation with the highest  $R^2$  value was preferred. Equations 1–8 developed for these situations are presented in Table 6, and the graphs prepared are shown in Fig. 6. The analyses of variance for the validation of the equations were performed, and the results are given in Table 7. In this test, a 95% level of confidence was chosen.

While the best relationship between dry density and  $HL_D$  is in the exponential function, the best relationship between dry

Fig. 4 Influence of specimen size on the HL in magmatic rock

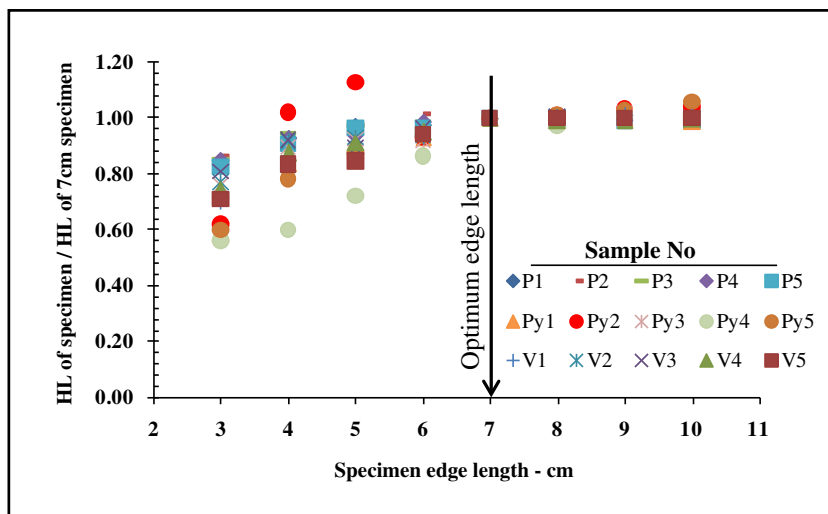


**Table 4** Some index and Leeb hardness properties of the rock samples

| Sample | $\rho_d$<br>(g/cm <sup>3</sup> ) | $n$ (%) | V <sub>p</sub> (km/s) | UCS (MPa) | HL <sub>D</sub> | HL <sub>S</sub> | Sample | $\rho_d$<br>g /<br>cm <sup>3</sup> | $n$ (%) | V <sub>p</sub> (km/s) | UCS (MPa) | HL <sub>D</sub> | HL <sub>S</sub> |
|--------|----------------------------------|---------|-----------------------|-----------|-----------------|-----------------|--------|------------------------------------|---------|-----------------------|-----------|-----------------|-----------------|
| P1     | 2.68                             | 1.17    | 4.27                  | 135.40    | 802.27          | 781.00          | Py26   | 1.91                               | 26.06   | 2.79                  | 30.70     | 357.33          | 297.17          |
| P2     | 2.61                             | 0.85    | 4.48                  | 161.25    | 872.27          | 868.00          | Py27   | 2.19                               | 12.13   | 3.35                  | 32.21     | 552.67          | 432.00          |
| P3     | 2.55                             | 1.77    | 4.33                  | 167.17    | 889.40          | 840.75          | Py28   | 1.88                               | 9.84    | 3.89                  | 29.78     | 550.67          | 439.20          |
| P4     | 2.61                             | 0.99    | 3.93                  | 158.96    | 881.47          | 861.00          | Py29   | 2.11                               | 12.30   | 3.90                  | 96.70     | 800.00          | 750.80          |
| P5     | 2.64                             | 0.92    | 5.43                  | 167.05    | 825.13          | 765.00          | Py30   | 1.84                               | 20.32   | 2.70                  | 39.10     | 512.33          | 365.60          |
| P6     | 2.71                             | 1.23    | 4.42                  | 194.60    | 874.60          | 794.86          | V1     | 2.64                               | 3.98    | 5.35                  | 140.38    | 781.53          | 695.33          |
| P7     | 2.62                             | 1.02    | 4.42                  | 141.56    | 892.67          | 847.00          | V2     | 2.36                               | 5.99    | 2.27                  | 111.22    | 800.93          | 770.50          |
| P8     | 2.66                             | 1.14    | 4.71                  | 176.00    | 887.33          | 825.25          | V3     | 2.32                               | 8.72    | 4.72                  | 116.33    | 713.93          | 735.50          |
| P9     | 2.66                             | 1.23    | 4.81                  | 106.40    | 880.67          | 837.00          | V4     | 2.30                               | 6.55    | 4.61                  | 144.01    | 809.00          | 702.25          |
| P10    | 2.63                             | 1.13    | 4.70                  | 96.25     | 895.40          | 838.75          | V5     | 2.26                               | 8.60    | 2.06                  | 63.24     | 651.67          | 519.00          |
| P11    | 2.64                             | 1.09    | 4.59                  | 153.80    | 870.00          | 823.00          | V6     | 2.46                               | 7.09    | 4.09                  | 95.39     | 706.67          | 635.60          |
| P12    | 2.66                             | 0.85    | 5.28                  | 155.40    | 861.00          | 802.63          | V7     | 2.28                               | 11.12   | 3.88                  | 66.69     | 772.33          | 649.67          |
| P13    | 2.85                             | 0.98    | 5.01                  | 123.46    | 842.00          | 715.00          | V8     | 2.04                               | 19.43   | 2.04                  | 21.36     | 467.33          | 380.40          |
| Py1    | 1.48                             | 26.59   | 1.88                  | 15.09     | 451.93          | 411.50          | V9     | 2.12                               | 9.50    | 2.38                  | 30.79     | 553.33          | 460.00          |
| Py2    | 1.83                             | 22.38   | 2.92                  | 30.96     | 501.27          | 369.80          | V10    | 2.06                               | 13.00   | 2.51                  | 22.15     | 575.67          | 385.67          |
| Py3    | 1.85                             | 19.72   | 1.76                  | 40.32     | 610.33          | 580.25          | V11    | 2.14                               | 16.11   | 3.53                  | 100.56    | 714.00          | 610.00          |
| Py4    | 1.42                             | 31.92   | 2.57                  | 20.26     | 383.53          | 326.00          | V12    | 2.27                               | 7.30    | 4.36                  | 65.20     | 743.33          | 637.17          |
| Py5    | 1.35                             | 37.36   | 2.08                  | 9.90      | 300.33          | 274.00          | V13    | 2.20                               | 10.70   | 3.60                  | 98.40     | 759.67          | 643.17          |
| Py6    | 1.75                             | 23.89   | 2.95                  | 48.63     | 580.33          | 505.25          | V14    | 2.32                               | 5.65    | 3.78                  | 60.60     | 784.00          | 652.33          |
| Py7    | 1.54                             | 24.81   | 2.30                  | 10.55     | 363.67          | 288.75          | V15    | 2.38                               | 4.81    | 4.91                  | 78.20     | 769.00          | 721.00          |
| Py8    | 1.30                             | 36.83   | 2.02                  | 7.57      | 258.00          | 187.00          | V16    | 2.48                               | 5.54    | 4.12                  | 59.88     | 791.00          | 719.67          |
| Py9    | 1.63                             | 25.57   | 2.58                  | 31.57     | 399.67          | 333.50          | V17    | 2.36                               | 7.11    | 4.82                  | 67.59     | 680.33          | 621.67          |
| Py10   | 1.78                             | 19.53   | 2.28                  | 48.38     | 508.33          | 458.75          | V18    | 2.51                               | 4.37    | 4.67                  | 64.94     | 772.33          | 700.67          |
| Py11   | 1.82                             | 26.21   | 2.69                  | 36.64     | 488.67          | 437.75          | V19    | 2.28                               | 7.16    | 3.97                  | 61.30     | 768.33          | 598.00          |
| Py12   | 1.42                             | 33.05   | 2.90                  | 27.27     | 247.33          | 299.60          | V20    | 2.25                               | 8.23    | 4.25                  | 63.85     | 759.00          | 541.00          |
| Py13   | 1.75                             | 21.09   | 2.45                  | 16.86     | 311.67          | 203.50          | V21    | 2.35                               | 5.16    | 4.10                  | 50.68     | 755.67          | 618.75          |
| Py14   | 1.49                             | 34.29   | 2.57                  | 9.52      | 324.67          | 265.80          | V22    | 2.34                               | 7.29    | 4.66                  | 85.35     | 674.00          | 567.50          |
| Py15   | 1.54                             | 28.45   | 2.49                  | 24.51     | 311.67          | 199.60          | V23    | 2.34                               | 6.30    | 4.76                  | 71.16     | 735.67          | 621.20          |
| Py16   | 1.66                             | 30.76   | 2.19                  | 15.68     | 321.67          | 251.80          | V24    | 2.30                               | 8.68    | 3.90                  | 83.63     | 748.67          | 649.75          |
| Py17   | 1.94                             | 14.84   | 2.64                  | 48.76     | 720.00          | 602.20          | V25    | 2.34                               | 8.37    | 3.95                  | 83.11     | 799.00          | 700.25          |
| Py18   | 1.82                             | 20.16   | 2.27                  | 32.00     | 648.67          | 581.00          | V26    | 2.34                               | 6.80    | 4.40                  | 91.68     | 744.00          | 667.75          |
| Py19   | 2.03                             | 15.32   | 2.65                  | 59.71     | 745.00          | 674.40          | V27    | 2.22                               | 12.30   | 3.57                  | 48.13     | 673.33          | 571.80          |
| Py20   | 1.75                             | 26.52   | 1.92                  | 12.30     | 378.67          | 268.60          | V28    | 2.43                               | 3.46    | 4.65                  | 89.60     | 768.67          | 686.00          |
| Py21   | 2.01                             | 12.67   | 2.57                  | 42.13     | 703.33          | 681.60          | V29    | 2.36                               | 6.87    | 2.14                  | 78.60     | 823.00          | 765.50          |
| Py22   | 1.84                             | 19.11   | 2.95                  | 39.62     | 547.67          | 497.75          | V30    | 2.38                               | 7.43    | 3.42                  | 68.97     | 722.67          | 693.40          |
| Py23   | 1.23                             | 34.89   | 2.04                  | 11.02     | 220.00          | 179.40          | V31    | 2.48                               | 1.64    | 4.72                  | 129.39    | 892.33          | 826.50          |
| Py24   | 1.86                             | 16.83   | 1.56                  | 13.78     | 365.00          | 246.60          | V32    | 2.46                               | 6.04    | 4.36                  | 100.47    | 769.67          | 626.75          |
| Py25   | 1.70                             | 26.27   | 2.43                  | 18.95     | 516.00          | 378.10          | V33    | 2.61                               | 3.49    | 5.38                  | 112.79    | 820.00          | 666.25          |

density and HL<sub>S</sub> is in the linear function. The  $R^2$  value between dry density and HL<sub>D</sub> and HL<sub>S</sub> is 0.85 and 0.79, respectively (Fig. 6a, b). HL values increase with increasing density value of rocks. A linear relationship was determined between porosity and HL values. While the  $R^2$  value between HL<sub>D</sub> and  $n$  is 0.87, the  $R^2$  value between HL<sub>S</sub> and  $n$  is 0.80 (Fig. 6c, d). HL<sub>D</sub> and HL<sub>S</sub> values decrease with the increasing porosity

value of the rock samples. The relationship between the P-wave velocity and HL values is shown in Fig. 6e, f. While the  $R^2$  value between HL<sub>D</sub> and V<sub>p</sub> is 0.57, the  $R^2$  value between HL<sub>S</sub> and V<sub>p</sub> is determined to be 0.54 (Fig. 6e, f). When the reason why the  $R^2$  is lower than other properties is examined, it is observed that some values deviated from the drawn chart. This is because, while HL value is directly related to the



**Table 5** Descriptive statistics of the data used in the analysis

| Variables                     | Data | Mean   | Std. deviation | Variance  | Minimum | Maximum |
|-------------------------------|------|--------|----------------|-----------|---------|---------|
| $\rho_d$ (g/cm <sup>3</sup> ) | 76   | 2.15   | 0.40           | 0.16      | 1.23    | 2.85    |
| $n$ (%)                       | 76   | 12.88  | 10.52          | 110.76    | 0.85    | 37.36   |
| V <sub>p</sub> (km/s)         | 76   | 3.51   | 1.10           | 1.20      | 1.56    | 5.43    |
| UCS (MPa)                     | 76   | 71.89  | 49.06          | 2406.52   | 7.57    | 194.60  |
| HL <sub>D</sub>               | 76   | 652.03 | 194.26         | 37,738.64 | 220.00  | 895.40  |
| HL <sub>S</sub>               | 76   | 571.40 | 197.81         | 39,126.91 | 179.40  | 868.00  |

surface properties of the rock, the V<sub>p</sub> value is associated with the rock’s internal structural properties (grain size, porosity, etc.).

An exponential relationship was determined between UCS and HL values. The R<sup>2</sup> values between HL<sub>D</sub> and UCS and HL<sub>S</sub> and UCS are found to be as 0.85 and 0.86, respectively. The HL value tends to increase with the increasing UCS values of rocks (Fig. 6g, h). The developed statistical models showed that it could be used confidentially in estimating the index values of rock samples for a 5% significance level ( $\alpha = 0.05$ ).

By evaluating the data of the magmatic rocks used in previous studies (Aoki and Matsukura 2008; Çelik and Çobanoğlu 2019; Hack et al. 1993; Kawasaki et al. 2002; Meulenkamp and Grima 1999; Verwaal and Mulder 1993; Yılmaz Güneş and Goktan 2019; Su and Momayez 2017; Gomez-Heras et al. 2020; Aldeeky et al. 2020, Çelik et al. 2020) and the data used in this study together, the relationship between UCS and HL was redefined. Considering all the data, the best R<sup>2</sup> (0.85) between UCS and HL<sub>D</sub> was obtained in the exponential function (Fig. 7; Table 8). Figure 7 indicates that

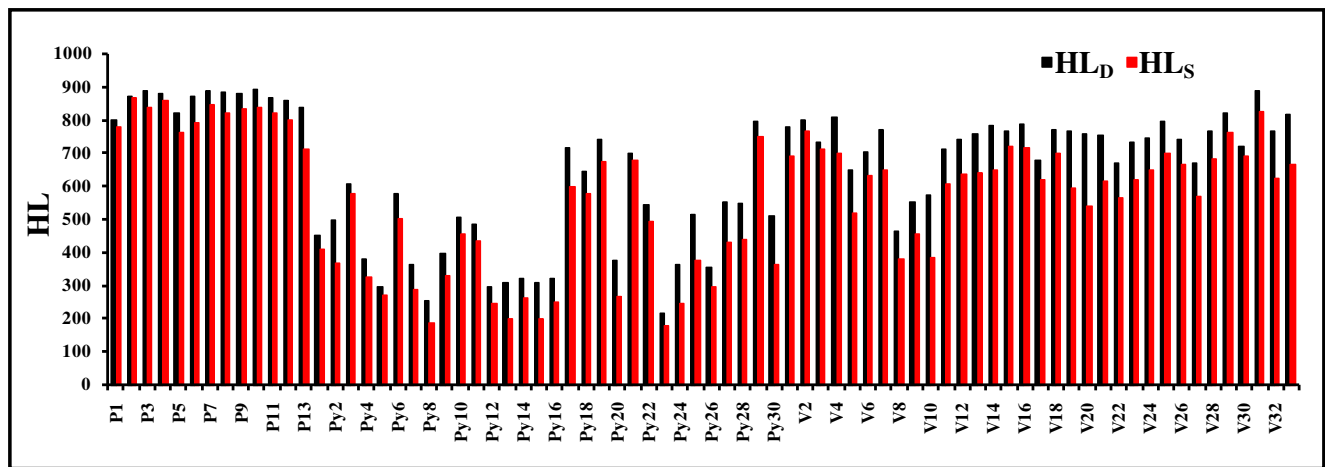


**Fig. 5** Comparison of the HL values measured in dry and saturated samples

**Table 6** Correlation between Leeb hardness vs. index values of the samples

|                              | Rock properties                     | Equation                      | R <sup>2</sup> | Equation no. |
|------------------------------|-------------------------------------|-------------------------------|----------------|--------------|
| HL <sub>D</sub>              | Dry density ( $\rho_d$ )            | $\rho_d = 1.124e^{0.001HL_D}$ | 0.85           | 1            |
|                              | Porosity ( $n$ )                    | $n = 45.77 - 0.050HL_D$       | 0.87           | 2            |
|                              | Ultrasonic velocity ( $V_p$ )       | $V_p = 0.72 + 0.004HL_D$      | 0.57           | 3            |
|                              | Uniaxial compressive strength (UCS) | $UCS = 4.076e^{0.004HL_D}$    | 0.85           | 4            |
| HL <sub>S</sub>              | Dry density ( $\rho_d$ )            | $\rho_d = 1.110 + 0.001HL_S$  | 0.79           | 5            |
|                              | Porosity ( $n$ )                    | $n = 39.99 - 0.047HL_S$       | 0.80           | 6            |
|                              | Ultrasonic velocity ( $V_p$ )       | $V_p = 1.176 + 0.004HL_S$     | 0.54           | 7            |
|                              | Uniaxial compressive strength (UCS) | $UCS = 5.783e^{0.003HL_S}$    | 0.86           | 8            |
| <sup>a</sup> HL <sub>D</sub> | Uniaxial compressive strength (UCS) | $UCS = 2.927e^{0.005HL_D}$    | 0.85           | 9            |

<sup>a</sup> Evaluation of the data obtained from this study and those in other studies

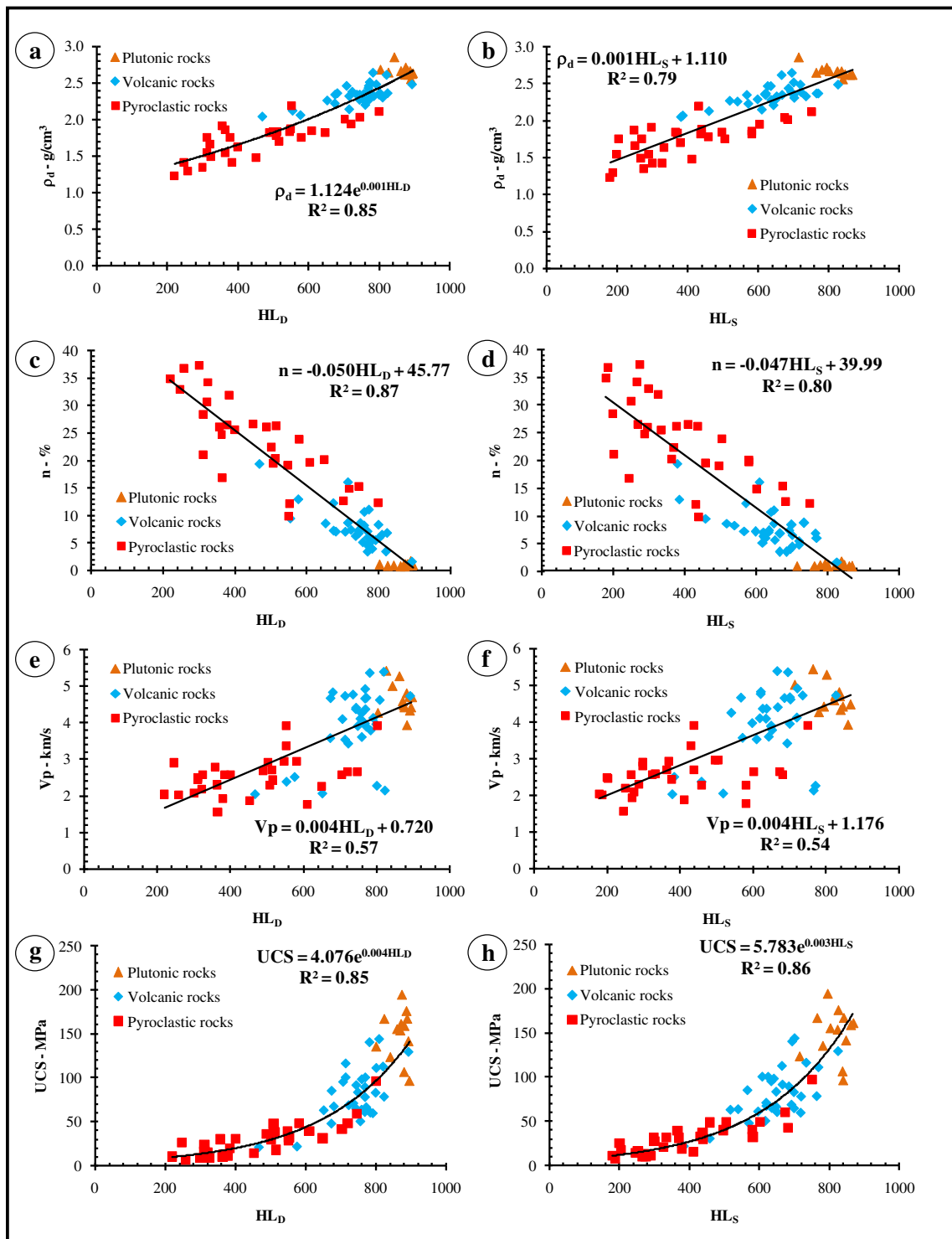


**Fig. 6** Correlation between HL and dry density (a, b); porosity (c, d); P-wave velocity (e, f); and uniaxial compressive strength (g, h)

when the HL value exceeds 850, the UCS values are scattered abruptly. In this case, it is not applicable to use HL in predicting UCS values of rocks. This relationship is formulated as given in Eq. 9 (Table 6). The analysis of variance for the validation of = Eq. 9 was performed, and the results are presented in Table 9.

Three equations were developed in the estimation of the UCS value of magmatic rocks by using saturated and dry HL values. Equations 4 and 8 are the equations obtained from the data of 76 samples used in this study, and the other is the equation obtained from 144 magmatic rock data used in this study and in previous studies (Eq. 9). The correlation

**Table 7** The variance analysis of the models

| Rock properties |          | $R^2$ | $t$ -test | $F$ -test | $p < 0.05$ |
|-----------------|----------|-------|-----------|-----------|------------|
| HL <sub>D</sub> | $\rho_d$ | 0.85  | 20.630    | 425.580   | 0.000      |
|                 | $n$      | 0.87  | - 21.971  | 482,746   | 0.000      |
|                 | $V_p$    | 0.57  | 9.975     | 99.509    | 0.000      |
|                 | UCS      | 0.85  | 20.358    | 414.467   | 0.000      |
| HL <sub>S</sub> | $\rho_d$ | 0.79  | 16.780    | 281.573   | 0.000      |
|                 | $n$      | 0.80  | - 16.968  | 287.922   | 0.000      |
|                 | $V_p$    | 0.54  | 9.354     | 87.496    | 0.000      |
|                 | UCS      | 0.86  | 20.977    | 440.050   | 0.000      |

equations developed for the estimation of the UCS value can be widely used in practice, and the UCS value of rock materials can be estimated with significant accuracy. By increasing the number of samples, equations that make estimations with higher accuracy can be developed.

### Conclusions

In the first stage of this study, the relationship between the sample size and HL values on 15 different rock samples belonging to 3 different rock groups was examined. In the second stage, the relationship between the index properties and HL values on 76 different magmatic rock samples was investigated. Based on the obtained analysis results, the following main conclusions were drawn:

- By analysing the Leeb hardness values of magmatic rocks measured in the laboratory, the minimum edge length of cubic samples was found to be 7 cm. Moreover, it was determined that as the strength value of magmatic rocks increases, the effect of sample size on HL value decreases.
- The HL value of magmatic rocks was affected by phenocrysts in sample P1 and volcanic rock fragments in

**Table 8** The statistical results of simple regression analysis (for 144 samples)

| Model           | Unstandardized coefficients |            | Standardized coefficients<br>Beta | $t$    | $p$   |
|-----------------|-----------------------------|------------|-----------------------------------|--------|-------|
|                 | $\beta$                     | Std. error |                                   |        |       |
| HL <sub>D</sub> | 0.005                       | 0.000      | 0.923                             | 28.520 | 0.000 |
| (Constant)      | 2.927                       | 0.328      |                                   | 8.913  | 0.000 |

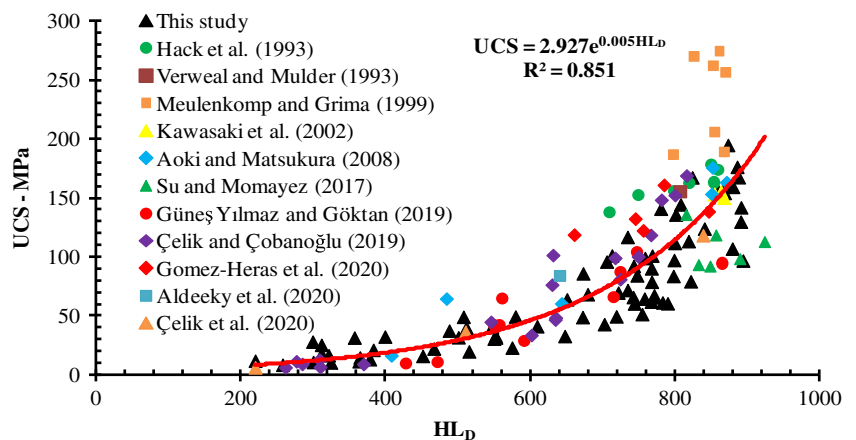
**Table 9** The variance analysis of the models (for 144 samples)

| Model      | Sum of squares | Degree of freedom | Mean square | $F$     | $p$   |
|------------|----------------|-------------------|-------------|---------|-------|
| Regression | 108.265        | 1                 | 108.265     | 813.366 | 0.000 |
| Residual   | 18.901         | 142               | 0.133       |         |       |
| Total      | 127.166        | 143               |             |         |       |

pyroclastic sample Py2. As the size of the grains on the measurement surfaces of the rocks increases, the amplitude of the fluctuations in the HL value increases.

- The best relationships between the HL<sub>D</sub> and HL<sub>S</sub> values of the samples and the index properties were generally determined as linear functions. The porosity gives the best relationship between the HL<sub>D</sub> value and index properties of rock samples with a determination coefficient of  $R^2$  of 0.87.
- While HL<sub>D</sub> and HL<sub>S</sub> values increase with increasing dry density and P-wave velocity, they decrease with the increase of porosity.
- The best relationship between HL<sub>D</sub> and HL<sub>S</sub> values and UCS values was defined as an exponential function, and the  $R^2$  values were found to be 0.85 and 0.86, respectively.
- When the data obtained from previous studies and this study was evaluated together, the best correlation

**Fig. 7** The comparison of data obtained from this study with those of other studies



relationship between HL and UCS was determined in the exponential function ( $R^2 = 0.85$ ).

The HL measurement is an NDT, basic, easy-to-apply, and inexpensive method for testing rocks. HL can be useful in rock groups where sampling is difficult. Furthermore, this method can yield essential results in determining the rock properties in historical structures where sampling is not possible due to conservation reasons and following the degradation processes. HL measurements can make a significant contribution to preliminary evaluations of engineering applications.

## Compliance with ethical standards

**Conflict of interest** The authors declare that they have no conflict of interest.

## References

- Aldeeky H, Al Hattamleh O, Rababah S (2020) Assessing the uniaxial compressive strength and tangent Young's modulus of basalt rock using the Leeb rebound hardness test. *Mater Constr* 70(340):e230. <https://doi.org/10.3989/mc.2020.15119>
- Alvarez Grima M, Babuška R (1999) Fuzzy model for the prediction of unconfined compressive strength of rock samples. *Int J Rock Mech Min Sci* 36:339–349. [https://doi.org/10.1016/S0148-9062\(99\)00007-8](https://doi.org/10.1016/S0148-9062(99)00007-8)
- André MF, Voltaire O, Vautier F, Roussel E, Phalip B, Morel D (2014) Impact of cement repointing on rates of sandstone decay in medieval churches of the French Massif Central. Geological Society, London, Special Publications 391:157–174. <https://doi.org/10.1144/sp391.4>
- Aoki H, Matsukura Y (2008) Estimating the unconfined compressive strength of intact rocks from Equotip hardness. *Bull EngGeol Environ* 67:23–29. <https://doi.org/10.1007/s10064-007-0116-z>
- Asiri Y (2017) Standardized Process for Filed Estimation of Unconfined Compressive Strength Using Leeb Hardness. Master, Dalhousie University
- Asiri Y, Corkum A, El Naggar H (2016) Leeb hardness test for UCS estimation of sandstone. Paper presented at the 69th Annual Canadian Geotechnical Conference, Vancouver, October 2016
- ASTM A956 (2012) Standard Test Method for Leeb Hardness Testing of Steel Products. ASTM International, West Conshohocken
- ASTM E494 (2010) Standard Practice for Measuring Ultrasonic Velocity in Materials. ASTM International, West Conshohocken
- Bieniawski ZT (1989) Engineering rock mass classifications: a complete manual for engineers and geologists in mining, civil, and petroleum engineering. Wiley
- Coombes MA, Feal-Pérez A, Naylor LA, Wilhelm K (2013) A non-destructive tool for detecting changes in the hardness of engineering materials: Application of the Equotip durometer in the coastal zone. *EngGeol* 167:14–19. <https://doi.org/10.1016/j.enggeo.2013.10.003>
- Corkum AG, Asiri Y, El Naggar H, Kinakin D (2018) The Leeb hardness test for rock: an updated methodology and UCS correlation. *Rock Mech Rock Eng* 51:665–675. <https://doi.org/10.1007/s00603-017-1372-2>
- Çelik SB, Çobanoğlu İ (2019) Comparative investigation of Shore, Schmidt, and Leeb hardness tests in the characterization of rock materials. *Environ Earth Sci* 78:554. <https://doi.org/10.1007/s12665-019-8567-7>
- Çelik SB, Çobanoğlu İ, Koralay T (2020) Investigation of the use of Leeb hardness in the estimation of some physical and mechanical properties of rock materials. *Pamukkale Univ J Eng Sci* 26:1385–1392. <https://doi.org/10.5505/pajes.2020.22747>
- Feal-Pérez A, Blanco-Chao R (2013) Characterization of abrasion surfaces in rock shore environments of NW Spain. *Geo-Mar Lett* 33: 173–181. <https://doi.org/10.1007/s00367-012-0300-4>
- Fener M, Ince I (2012) Influence of orthoclase phenocrysts on point load strength of granitic rocks. *EngGeol* 141-142:24–32. <https://doi.org/10.1016/j.enggeo.2012.05.003>
- Gomez-Heras M, Benavente D, Pla C, Martinez-Martinez J, Fort R, Brotons V (2020) Ultrasonic pulse velocity as a way of improving uniaxial compressive strength estimations from Leeb hardness measurements. *Constr Build Mater* 261:119996. <https://doi.org/10.1016/j.conbuildmat.2020.119996>
- Hack H, Hingira J, Verwaal W (1993) Determination of discontinuity wall strength by Equotip and ball rebound tests. In: *Int J Rock Mech Min Sci Geomech, Abstracts*, Pergamon Press, pp 151–151
- Kawanishi T, Hirata T, Yashiro T, Kawai K (2019) A simple method to evaluate the depth of concrete degradation by fire. *J AdvConcrTechnol* 17:639–647
- Kawasaki S, Tanimoto C, Koizumi K, Ishikawa M (2002) An attempt to estimate mechanical properties of rocks using the Equotip hardness tester. *J Japan Soc EngGeol* 43:244–248 (in Japanese)
- Kovler K, Wang F, Muravin B (2018) Testing of concrete by rebound method: Leeb versus Schmidt hammers. *Mater Struct* 51:138. <https://doi.org/10.1617/s11527-018-1265-1>
- Leeb D (1979) Dynamic hardness testing of metallic materials. *NDT Int* 12(6):274–278
- Lee JS, Smallwood L, Morgan E (2014) New application of rebound hardness numbers to generate logging of unconfined compressive strength in laminated shale formations. In: 48th US rock mechanics - geomechanics symposium 2:972–978.
- Meulenkamp F, Grima MA (1999) Application of neural networks for the prediction of the unconfined compressive strength (UCS) from Equotip hardness. *Int J Rock Mech Min Sci* 36:29–39. [https://doi.org/10.1016/S0148-9062\(98\)00173-9](https://doi.org/10.1016/S0148-9062(98)00173-9)
- Mol L, Gomez-Heras M (2018) Bullet impacts and built heritage damage 1640–1939. *Heritage Sci* 6:35. <https://doi.org/10.1186/s40494-018-0200-7>
- Mol L, Viles HA (2012) The role of rock surface hardness and internal moisture in tafoni development in sandstone. *Earth Surf Processes Landforms* 37:301–314. <https://doi.org/10.1002/esp.2252>
- NBG (1985) Engineering geology and rock engineering, Handbook no. 2. Norwegian Group for Rock Mechanics (NBG), Norway, 2 edn., Trondheim, Norway
- Schmid R (1981) Descriptive nomenclature and classification of pyroclastic deposits and fragments: recommendations of the international union of geological sciences subcommission on the systematics of igneous rocks. *Geology* 9:41–43 The Geological Society of America. Boulder
- Su O, Momayez M (2017) Correlation between Equotip hardness index, mechanical properties and drillability of rocks. *Dokuz Eylul Univ J SciEng* 19(56):519–531
- Streickeisen A (1979) Classification and nomenclature of volcanic rock lompophyres, corbanatites and millitic rocks. *Geology* 7:331–335
- TS EN-1936 (2010) Natural stone test methods - Determination of real density and apparent density and of total and open porosity. Turkish Standards Institution, Turkey
- TS EN-1926 (2007) Natural stone test methods - Determination of uniaxial compressive strength. Turkish Standards Institution, Turkey
- Verwaal W, Mulder A (1993) Estimating rock strength with the Equotip hardness tester. In: *Int J Rock Mech Min Sci Geomech Abstracts*, vol 6. Elsevier Science, pp 659–662
- Viles H, Goudie A, Grab S, Lalley J (2011) The use of the Schmidt Hammer and Equotip for rock hardness assessment in

- geomorphology and heritage science: a comparative analysis. *Earth Surf Processes Landforms* 36(3):320–333. <https://doi.org/10.1002/esp.2040>
- Wakasa S, Matsuzaki H, Tanaka Y, Matsukura Y (2006) Estimation of episodic exfoliation rates of rock sheets on a granite dome in Korea from cosmogenic nuclide analysis. *Earth Surf Processes Landforms* 31:1246–1256. <https://doi.org/10.1002/esp.1328>
- Wang Y, Pei Q, Yang S, Guo Q, Viles H (2020) Evaluating the condition of sandstone rock-hewn cave-temple façade using in situ non-invasive techniques. *Rock Mech Rock Eng.* 53:2915–2920. <https://doi.org/10.1007/s00603-020-02063-w>
- Wilhelm K, Viles H, Burke O, Mayaud J (2016) Surface hardness as a proxy for weathering behaviour of limestone heritage: a case study on dated headstones on the Isle of Portland, UK. *Environ Earth Sci* 75:931. <https://doi.org/10.1007/s12665-016-5661-y>
- Yilmaz Güneş N, Goktan RM (2019) Comparison and combination of two NDT methods with implications for compressive strength evaluation of selected masonry and building stones. *Bull EngGeol Environ* 78: 4493–4503. <https://doi.org/10.1007/s10064-018-1382-7>